Photodissociation of Noble Metal-Doped Carbon Clusters

B. W. Ticknor, B. Bandyopadhyay, and M. A. Duncan*

Department of Chemistry, University of Georgia, Athens, Georgia 30602-2556

Received: September 4, 2008; Revised Manuscript Received: October 7, 2008

Noble metal carbide cluster cations (MC_n^+, M = Cu, Au) are produced by laser vaporization in a pulsed molecular beam and detected with time-of-flight mass spectrometry. Copper favors the formation of carbides with an odd number of carbon atoms, while gold shows marked drops in ion intensity after clusters with 3, 6, 9, and 12 carbons. These clusters are mass selected and photodissociated at 355 nm. Copper carbides with an odd number of carbons fragment by eliminating the metal from the cluster; for the small species it is eliminated as Cu^+ and for the larger species it is lost as neutral Cu. Copper carbides with an even number of carbons also lose the metal, but in addition to this they eliminate neutral C_3. This even−odd alternation, with the even clusters having mixed fragments, holds true for clusters as large as CuC_{30}^+. No loss of C_2 is observed for even the largest clusters studied, indicating that fullerene formation does not occur. The gold carbide photodissociation data closely parallel that of copper, with even clusters losing primarily C_3 and odd ones losing gold. Comparisons to known carbon cluster ionization potentials give some insight into the structures of carbon photofragments. DFT calculations performed on CuC_{3-11}^+ allow comparisons of the energetics of isomers likely present in our experiment, and metal−carbon dissociation energies help explain the even−odd alternation in the fragmentation channels. The simplest picture of these metal-doped carbides consistent with all the data is that the small species have linear chain structures with the metal attached at the end, whereas the larger species have cyclic structures with the metal attached externally to a single carbon.

Introduction

Transition metal carbides are important in areas such as ceramics, catalysis, astrophysics, and surface science,[1−5] and nanoclusters of these materials have also generated considerable interest. Depending on the relative concentrations of metal and carbon, a variety of structural patterns are possible for these systems. The linear chain and cyclic ring structures of small carbon clusters are well-known,[6,7] as are the fullerene cages of larger carbon clusters.[8,9] Small carbides seen in early mass spectrometry experiments were thought to form chain and ring structures like the small pure carbon clusters.[10−15] In larger systems, the reactions of early transition metals with hydrocarbons led to the discovery of three-dimensional carbide cages called metallo-carbohedrenes, or "met-cars", along with their cubic analogues known as metal carbide "nanocrystals".[16−21] The initial mass spectrometry experiments were followed by ion mobility[22] and spectroscopy experiments,[23−25] as well as many theoretical studies,[26−44] to try to establish the structures of these and other carbide clusters. The work on met-cars and nanocrystals stimulated additional experiments on a variety of other metal−carbon clusters.[45−57] Much larger carbon clusters such as fullerenes are also known to bind metals to form metallofullerenes, with endohedral,[8,9,58,59] exohedral,[60−66] or networked[62,64] structures. In all of these carbide systems, the determination of electronic structure, geometry, and stability is problematic. Photodissociation studies, like those described here for noble metal (Cu, Au) carbide clusters, provide a convenient probe of the structures and stabilities of these fascinating systems.

Metal carbide clusters have been studied for many years in mass spectrometry. The earliest experiments utilized high-temperature Knudsen ovens and variable energy electron impact ionization to record ionization thresholds and estimate dissociation energies for these species.[10−13] Secondary ion mass spectrometry (SIMS) was also used to study anions and cations produced from fast atom bombardment of bulk metal carbide samples,[14] and carbides were also produced in some of the earliest laser vaporization experiments.[15] In 1992, Castleman and co-workers used laser vaporization in conjunction with hydrocarbon plasma reactions to discover metallocarbohedrene clusters, commonly called "met-cars", which have the M_8C_{12} stoichiometry.[16] Additional studies by Duncan and co-workers revealed the larger cubic nanocrystals having the $M_{14}C_{13}$ stoichiometry.[17] These clusters, which form primarily from the early transition metals, have been studied with photodissociation,[17,18] collision-induced dissociation (CID),[20] metastable decay,[21] and ion mobility experiments.[22] More recently, mass spectrometry has been used to study carbides from oven sources,[45] laser photolysis of organometallic vapor,[46] as well as laser vaporization sources.[47−57] The initial studies focused on the early transition metals, which are more reactive with hydrocarbon gases and produce met-cars species more efficiently. Carbides of less reactive metals (bismuth, antimony, nickel, cobalt, and copper) have been produced with composite samples (metal film-coated carbon rods).[49] Because they are more difficult to produce, noble metal carbides have been the subject of only a few studies.[45,49,50,52] In the present study, we use metal film-coated carbon rods to produce and study copper and gold carbide clusters.

Spectroscopy experiments on carbides that might reveal their structures are not common, but some progress has been made in this area. Graham and co-workers recorded vibrational spectra of neutral carbides of titanium, chromium, cobalt, and nickel in argon matrices,[51] and recently Vala and co-workers used similar methods to study CuC_3.[52] Metha and co-workers studied

* Corresponding author. E-mail: maduncan@uga.edu. Fax: 706-542-1234.

10.1021/jp807867r CCC: $40.75
Published on Web 11/08/2008

tantalum and niobium carbides with threshold ionization spectroscopy and DFT, determining ionization potentials (IPs) and corresponding structures.[53] Anionic metal carbide clusters have also been studied in the gas phase by photoelectron spectroscopy (PES).[54−57] PES experiments, along with numerous theoretical studies, have investigated the structures of both met-cars and nanocrystals.[23] Resonance-enhanced infrared multiphoton ionization with a tunable free electron laser was employed to measure the vibrational spectra for met-cars and nanocrystal carbides of several metals,[24,25] confirming the cubic structure for the nanocrystal and the general nature of the cage formed for the met-cars. The IR spectra of the titanium carbide nanocrystals led to the assignment of the 21 μm line seen in stellar atmospheres.[25] Unfortunately, except for the matrix isolation work on CuC_3,[52] there is no spectroscopic data for noble metal carbides.

Theoretical studies on metal carbide clusters are numerous. As mentioned above, extensive computational work has been conducted on the met-cars cages themselves or on smaller units believed to be building blocks for these systems.[26−40] As with the experimental work, much of the theory focuses on the early transition metals, which form the met-cars and nanocrystal stoichiometries most prominently. Unlike the other transition metal carbides, theoretical work on noble metal systems is extremely sparse. Carbohedrene structures of copper[26] and cubic clusters of copper, silver, and gold[41] have been investigated. Pyykkö and co-workers[42] and Peterson and co-workers[43] have studied small gold carbides in the larger context of gold chemistry. Finally, a cage structure with a tetrahedral C_5 radical surrounded by a spherical Au_{12} layer has been proposed by Naumkin.[44]

Photodissociation is a convenient experimental probe of cluster structure when spectroscopic information is not available. This is true for small clusters of pure carbon, where mass spectrometry shows interesting distributions[67−73] but optical spectroscopy methods have not yet been applied to many systems. Photodissociation[74−78] and collisional dissociation[79−81] studies have documented the elimination of C_3 in the small size regime and found that the loss of C_2 is characteristic of the larger clusters. In coordination with ion mobility measurements that reveal three-dimensional structures,[82] the C_3 elimination channel can be assigned to linear chain and cyclic structures and the C_2 loss is associated with fullerene cages. Other mass-selected cluster photodissociation studies have been applied to a variety of metal compound clusters. Our group has investigated metal−oxide,[83] silicon−carbide,[84] and metal−silicon[85] clusters by this method. However, photodissociation has not yet been applied to copper or gold carbides.

Many questions remain about the geometries, electronic structure, and bonding of small metal carbide clusters. If metal−carbon bonding is strong, integrated structures may be formed like the met-cars or carbide nanocrystal systems, whereas if carbon−carbon bonding is stronger, metal adducts to stable carbon chain, ring, or cage structures may dominate. Almost no experimental information exists on the carbides of the noble metals, and only a few theoretical studies address clusters of this type. The present study applies mass spectrometry and laser photodissociation techniques to copper and gold carbides. Cluster formation and fragmentation patterns, coupled with DFT calculations, give insight into the structures and bonding in these systems.

Experimental Section

The laser vaporization source and pulsed molecular beam machine used here have been described previously.[17,18,49,83−85] Coatings of copper or gold are prepared by oven vapor deposition on 0.5 in. carbon rods (Glass Supply).[49,85] The film-coated rod samples are transferred to the molecular beam machine for cluster experiments. In the source chamber of the molecular beam machine, the second harmonic (532 nm) of a Spectra Physics Nd:YAG laser (Quanta Ray GCR-11) is used to vaporize the rotating and translating rod. Helium (60 psi backing pressure) is pulsed with a Series 9 General Valve through the sample rod holder. The laser ablates the metal film and penetrates through it to ablate the underlying carbon. Clusters grow in the ensuing plasma and in the gas flow after this. The relative concentration of metal and carbon depends on the metal film thickness and the laser power, while the stability of the source also depends on the uniformity of the film thickness along the length of the rod. In experiments on larger clusters, a growth channel 0.5 in. long with a diameter of 5 mm is attached to the rod holder to promote aggregation. The molecular beam is skimmed into a differentially pumped chamber, where the cations grown in the source are pulse-extracted into a reflectron time-of-flight mass spectrometer. For photodissociation experiments, the cluster of interest is mass selected by pulsed deflection plates. The selected ion packet is then excited by the third harmonic (355 nm) of an Nd:YAG laser (Spectra Physics DCR-3) in the turning region of the reflectron. The photofragments are reaccelerated, mass separated in the second flight tube, and detected with an electron multiplier tube and a digital oscilloscope (LeCroy 9310A). Photodissociation studies were performed at laser powers between 6 and 50 mJ/pulse with an unfocused laser spot with an area approximately 1 cm^2.

To explore the structure and energetics in the small copper carbide clusters, geometry optimizations were performed by using density functional theory (DFT) computations with the Gaussian 03W program.[86] The B3LYP[87,88] functional with the 6-311+G(d,p)[89] basis set was used for carbon, and the LanL2DZ[90,91] basis set containing an effective core potential was used for copper. This method has been applied recently by Largo and co-workers on a variety of metal carbon systems.[39] Their work has shown that the B3LYP method has reasonable success in predicting ground states and low-lying excited states when compared to more computationally expensive methods such as QCISD or CCSD(T). The minimum energy structures, energies, and vibrational frequencies were computed for copper carbides CuC_{3-11}^+ and their corresponding neutral species, and these data are reported in the Supporting Information.

Results and Discussion

Figure 1 shows mass spectra collected with a copper/carbon sample. The upper trace shows the spectrum obtained using a holder with a 0.25 in. long by 2 mm diameter channel beyond the vaporization point, while the lower trace shows that obtained when an additional 0.5 in. long, 5 mm diameter channel section is added. The longer growth channel allows the formation of larger carbide and pure carbon clusters, as the lower trace shows. The doublet seen for clusters containing copper is due to its two isotopes, which are only resolved in the lower mass range. By far the largest peak in each spectrum under all conditions (excluding the atomic ion, not shown) corresponds to the CuC_3^+ cluster (hereafter 1/3). In fact, the 1/1 and 1/2 ions are not detected. There is a noticeable preference for carbides with an odd number of carbon atoms, particularly in the upper trace. In the lower trace, using the longer growth channel, the alternation is less noticeable and the even-numbered clusters are present in reasonable intensity. Additionally, in both mass spectra, pure

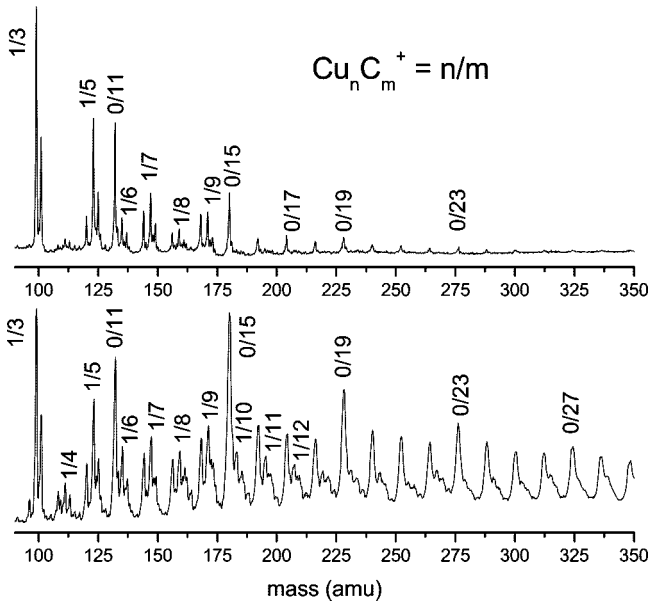

Figure 1. Mass spectra of copper carbide clusters formed in a helium expansion. The upper trace shows the cluster distribution from an expansion out of a rod holder. The lower trace shows the cluster distribution with a 0.5 in. growth channel attached to the end of the rod holder.

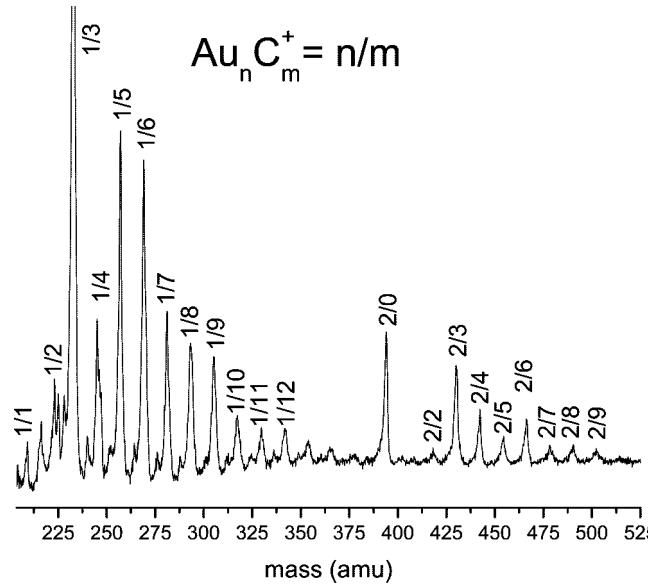

Figure 2. Mass spectrum of gold carbide clusters. The 1/3 peak is off scale.

carbon clusters are produced in significant quantities, as expected from the relative amount of carbon to copper present in the plasma vapor. Carbon is ablated more efficiently than metal and aggregates with itself efficiently, and with the use of the longer growth channel, pure carbon clusters out to C_{60}^+ are produced. The growth of the desired carbide species thus depends on optimizing the amount of metal versus carbon. The relative concentration of metal can be controlled roughly by adjusting the sample rod rotation rate. Rapid rotation provides a fresh surface for each laser shot, thus increasing the amount of metal in the vapor, leading to stronger carbide signals. Conversely, slower rotation favors the formation of pure carbon clusters. The mass spectra in Figure 1 were collected with a relatively fast rod rotation.

Several previous mass spectrometry studies on copper carbide clusters have been reported. Yamada and Castleman used a gas aggregation source that reacted copper vapor with acetylene (C_2H_2) gas dissociated over a hot filament and reported clusters with near stoichiometric ratios of metal to carbon.[45] That experiment favored the formation of clusters with multiple copper atoms. The copper concentration was evidently quite high, as pure copper clusters as large as Cu_{21}^+ were observed, and the smallest carbide observed was 3/2. Additionally, they saw only clusters containing an even number of carbon atoms. However, the carbon source in that experiment was acetylene, so the formation of carbides with C_2 adducts is perhaps not surprising. In a later study, Reddic and Duncan used laser vaporization of a film-coated carbon rod like that employed here to produce copper carbide clusters.[49] In that study, the 1/3 species was also prominent, while 1/1 and 1/2 were not seen, consistent with the results here. However, the spectra obtained in that study did not exhibit the strong even−odd alternation seen here.

The mass spectra shown here for copper carbides are also clearly different from those seen previously for pure carbon clusters. This suggests that, even though carbon is present in significantly higher concentration than copper, the carbon clusters are not simply forming in their usual distribution and then adding metal with equal probability to form the carbides. Previous mass spectrometry experiments on carbon cations exhibit enhanced abundances for C_3^+, C_7^+, C_{11}^+, C_{15}^+, and C_{19}^+.[67−78] The nascent distribution for the neutrals is difficult to measure, but C_3 is by far the most abundant species, and C_{10}, C_{12}, and C_{14} are also prominent.[72,73] While we do observe C_{11}^+, C_{15}^+, and C_{19}^+ with somewhat enhanced abundances, neither the cation nor the neutral carbon species seen previously correspond to the abundant carbides seen here. The presence of copper in the laser plasma affects the growth of the mixed clusters and their distribution.

It is tempting to speculate on the source of the even−odd alternation seen here in the abundant carbides because pure carbon clusters have also been found to exhibit some even−odd variations in properties.[6,7] If the growth mechanism here involves copper ions reacting with small carbon clusters (reasonable because the IP of copper is much lower than those of carbon or small carbon clusters), then the electronic structure of the carbon clusters may influence their tendency to add copper. For example, CuC_3^+ is the largest mass peak in these spectra and C_3 is by far the most abundant neutral cluster of pure carbon,[73] suggesting that $Cu^+ + C_3$ could play a role in the growth here. In general, small carbon species with an odd number of atoms (C_3, C_5, C_7, C_9) have linear $^1\Sigma_g^+$ ground states, while those with an even number of carbon atoms (C_4, C_6,C_8) tend to have cyclic ^1A_g or $^1A_1'$ ground states, with $^3\Sigma_g^-$ linear states lying slightly higher in energy.[6,7,73] The cumulenic bonding (:C═C···C═C:) in the odd-numbered linear singlet states leads to lone pairs of electrons on the ends of the chains that may be available for a dative type bond with the copper ion. The cyclic singlet or even-numbered linear triplet states would not have these same electron pairs, which may explain the preference for the odd CuC_n^+ species. This is also consistent with the lack of carbides larger than CuC_9^+ under some conditions (upper trace, Figure 1) despite the presence of larger pure carbon clusters. C_{10} and larger clusters favor cyclic structures by a substantial amount of energy,[6,7] and the ring isomers may not bond as efficiently to copper. Ion mobility studies have also suggested that linear carbon chains are more reactive than the cyclic structures.[82]

Figure 2 shows the mass spectrum collected for a carbon rod coated with gold. Pure carbon and mixed gold carbide clusters

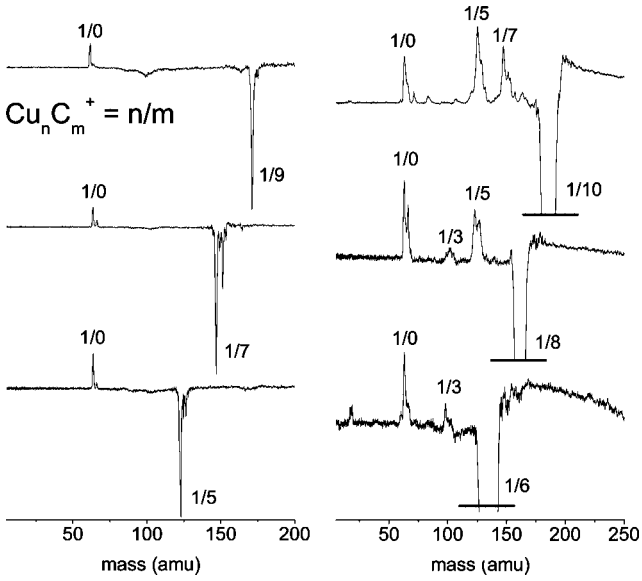

Figure 3. Photodissociation mass spectra of copper carbide clusters CuC_{5-10}^+ at 355 nm.

are both produced. In the lower mass region (not shown) the carbon distribution is peaked at C_{11}^+, and is similar to a pure carbon cluster distribution measured without metal. The mass spectrum shown was collected without a growth channel. When a growth channel is used, the intensity of the pure carbon clusters is so great that the gold carbide peaks cannot be detected. As with the copper, the 1/3 cluster ion produces by far the most intense peak in the spectrum, but both 1/1 and 1/2 are present here in small amounts. After 1/3, the 1/5 and 1/6 are the more abundant carbide peaks containing one gold atom. In behavior not seen for copper, clusters with two gold atoms and multiple carbons are also formed, e.g., 2/3, 2/4, and 2/6. The gold carbide mass peaks do not exhibit the even−odd alternation in intensity seen for the copper carbides. Instead, they display a somewhat noticeable decrease in local intensity after clusters with 3, 6, 9, and 12 carbon atoms. Again, the appearance of the mass spectrum is very different from that seen for pure carbon cations, so the presence of the gold changes the cluster distribution.

To our knowledge, there is only one previous mass spectrometry study on gold carbides. In the reactions of gold and its cluster cations with hydrocarbons, Gibson observed the formation of small gold carbides.[50] He saw no formation of AuC_n^+ clusters, apparently because Au^+ is not reactive enough to catalyze dehydrogenation and dehalogenation reactions. The gold dimer and larger cation clusters were reactive with various hydrocarbons. Carbon atoms and dimers attached to gold clusters were the most common reaction products, but carbides as big as 3/7 were produced under some conditions. However, there was no noticeable preference for any particular cluster size or stoichiometry in these data.

To further explore their structure and bonding, we have mass selected these copper and gold carbides and investigated them with photodissociation at 355 nm (3.49 eV). Figures 3−8 show photodissociation mass spectra for selected copper and gold carbides, and Table 1 presents the major fragmentation channels detected for all the clusters studied. The photodissociation data are accumulated by monitoring the mass spectrum with the photodissociation laser on and again when it is off. The two spectra are subtracted from each other, generating a difference spectrum. The negative-going peak represents the depletion of the parent ion, while the positive peaks correspond to the

TABLE 1: The Stoichiometries of Major Noble Metal Carbide Cluster Photofragments ($M_nC_m^+ = n/m$) Detected with 355 nm[a]

parent cation	fragment ions	
cluster	Cu	Au
1/3	**Cu**$^+$	**Au**$^+$
1/4	**Cu**$^+$	**Au**$^+$
1/5	**Cu**$^+$	**Au**$^+$
1/6	1/3, **Cu**$^+$	**1/3**, Au$^+$
1/7	**Cu**$^+$	1/4, **Au**$^+$, 0/7
1/8	1/5, 1/3, **Cu**$^+$	**1/5**, 1/3, 1/0, 0,8
1/9	**Cu**$^+$	1/6, 1/3, Au$^+$, **0/9**, 0/7, 0/6, 0/5
1/10	1/7,1/5,**Cu**$^+$	
1/11	1/8, **0/11**, Cu$^+$	
1/12	**1/9**, 1/7, 0/12, 0/11, Cu$^+$	
1/13	1/10, **0/13**, 0,10, Cu$^+$	
1/14	1/11, **0/14**, 0/11, Cu$^+$	
1/15	1/12, **0/15**, 0/12, Cu$^+$	
1/16	**1/13**, 1/11, 0/16, 0/11, Cu$^+$	
1/18	1/15, **0/18**, 0/15, 0,13, Cu$^+$	
1/20	1/17, **0/20**, 0/19, 0/18, 0/17, 0/15, Cu$^+$	
1/27	**0/27**, 0/24, 0/22, 0/19, 0/18, 0/16, 0/15, 0/14, 0/11	
1/28	1/25, **0/28**, 0/25, 0/23, 0/19, 0/15	
1/30	1/27, **0/30**, 0/28 - 0/14	
1/36	0/36, 0/31, 0/23 − 0/10 (**0/15 most intense**)	
1/43	0/43, 0/40, 0/38, 0/27, 0/23 − 0/10 (**0/19, 0/15 most intense**)	

[a] The fragments listed in bold were the most prominent.

charged photofragments produced. In principle, the combined integrated areas of the fragment peaks should equal the area of the parent ion depletion peak. Unfortunately, this is not always true because of the noise in the cluster source and the imperfect focusing of different masses. Because of this, the depletion of the parent ion is sometimes greater than the fragment ion intensities. For selected photodissociation mass spectra the parent ion is presented off scale to show the fragment ions in greater detail.

The photodissociation processes seen here are likely the result of multiphoton absorption. The dissociation energies are only known for a few selected species (see below), but their binding is expected to be comparable to, or greater than, the photon energy. Likewise, we do not know the wavelength dependence of absorption for any of these clusters, nor their dissociation efficiency. In each case, we use enough laser power to produce detectable fragment ion signals, but the power required is often quite high (10−20 mJ/pulse; unfocused). The limited range of laser powers for which signals can be detected, and the inherent noise in the cluster source, preclude meaningful studies of the laser power dependence. Therefore, we cannot make reliable conclusions about the number of photons absorbed or the corresponding energy that leads to photodissociation. Instead, we focus on the nature of the photofragments formed and the trends for the series of clusters studied.

Figure 3 shows the photodissociation mass spectra for small CuC_n^+ ($n = 5-10$) clusters. The clusters containing an odd number of carbon atoms are on the left side of the figure, while those with an even number of carbons are on the right. As shown, the odd-carbon species (1/5, 1/7, 1/9) all have only one charged photofragment, and that is the copper ion Cu^+. By mass conservation, the missing neutral fragment(s) corresponding to this could be the corresponding intact neutral carbon cluster fragment, C_n, or any one of several possible $C_{m<n}$ species all the way down to atoms. Because we only detect the charged species, we cannot make any definitive statement about the neutral fragments. However, for the odd-carbon species, we see

no intermediate $CuC_{m<n}$ ions, and further dissociation of neutral carbon clusters beyond the elimination of the metal would require significantly more energy. It is therefore most likely that these fragmentation processes correspond to simple elimination of the copper. Regardless of the carbon fragments, it makes sense that the copper atom, if it is eliminated by itself, is detected with a charge. Its ionization potential (7.73 eV)[92] is lower than those of most small carbon clusters (~8.8 eV and higher),[73] and the lowest energy fragmentation process results in the charge on the lowest IP species.

The simple fragmentation pattern seen for these odd-carbon carbides suggests that their structure is that of a carbon framework with an attached copper, and that the binding of the copper to the system is weaker than the carbon−carbon binding. This makes sense for several reasons. Carbon is generally easier to vaporize than metal, and therefore its concentration in the plasma is likely to be greater than that of copper. This concentration bias would favor the faster initial growth of carbon clusters, perhaps followed by the addition of metal. Copper−carbon bonds are also likely weaker than carbon−carbon bonds. In the case of the neutral diatomics, the dissociation energies have been calculated to be 5.8 eV for C_2 and 2.54 eV for CuC.[93,94] The corresponding values for the ions are 4.7 eV for C_2^+ and 2.02 eV for CuC^+.[93,94] For larger species, the dissociation energy of CuC_2 (to form Cu + C_2) has been calculated to be 3.42 eV for the linear isomer and 3.71 eV for the cyclic isomer,[39e] and the values for CuC_2^+ (to form Cu^+ + C_2) are 1.57 and 1.52 eV, respectively.[39h] Compared to this, the dissociation energy of C_9^+ into C_6^+ + C_3 has been measured by CID to be 5.7 eV.[79] In general, fragmenting a copper−carbon bond should be a lower energy process than fragmenting a carbon−carbon bond. In photodissociation processes on the ground electronic state, the weakest bond is expected to break first, which here would likely be the bond between the metal and the carbon. The simplest explanation for the odd-carbon dissociation processes shown in Figure 3, therefore, is that copper ion is eliminated, leaving a neutral carbon cluster behind.

Figure 3 also shows the photodissociation mass spectra for the even-numbered 1/6, 1/8, and 1/10 clusters. A prominent fragment for each of these species is again the copper atomic ion. However, in contrast to the odd-numbered species discussed above, these ions also produce metal carbide fragments: 1/6 fragments to 1/3, 1/8 fragments to 1/5 and 1/3, and 1/10 fragments to 1/7 and 1/5. It should also be noted that for some clusters (1/10, for example), small peaks present in the background correspond to fragmentation of pure carbon species not completely rejected by the mass selection which were still present in the reflectron together with the desired ion. Laser timing studies show that these peaks are not from the cluster of interest. As noted above, we only detect charged fragments, and cannot be sure about the missing neutral masses implied here. With multiple fragment ions, we also cannot be sure whether these come directly from the parent in multiple parallel processes or whether they come by sequential processes. However, if we assume minimum fragmentation in the neutrals, consistent with the lowest energy pathways, the neutral leaving groups suggested here are C_3 and C_5, respectively. The atomic Cu^+ fragment could also come either directly from the parent ion by elimination of a C_n neutral or in a sequence, such as $CuC_6^+ \rightarrow CuC_3^+ \rightarrow Cu^+$. C_3 is known to be a very stable neutral species[6,7] and it is a common neutral photofragment from dissociation of pure carbon cluster ions in about this same size range.[74−81] C_5 is also a common fragment from pure carbon clusters, but its production is only significant for larger sizes, beginning at C_{15}^+.[74,78] Although the full details of the dissociation mechanism cannot be determined, it is clear that these even-numbered species fragment differently from the odd-numbered ones. The even-numbered species tend to break carbon−carbon bonds and not only metal−carbon bonds. Because they survive in competition with carbon−carbon bonds, the metal−carbon bonds in these systems must be stronger than those in the odd-numbered clusters.

The appearance of mixed fragments for these clusters may also reflect the enhanced stability of 1/3, 1/5, and 1/7 as cations, which are also seen in the mass spectra. This process may be driven by the fact that simultaneously losing neutral C_3 or C_5 and forming 1/3, 1/5, or 1/7 are together energetically favorable. Another possible structure for 1/6 and 1/8 is the metal ion attached to two separate C_3 units or one C_3 and one C_5 unit. These structures seem unlikely because copper would not be expected to form multiple bonds. However, as mentioned above, C_3 and C_5 are known to be stable neutral fragments. The photodissociation data alone cannot confirm or disprove any of these possible structures.

Figure 4 shows photodissociation mass spectra for the 1/11, 1/12, and 1/13 copper carbide clusters. The fragmentation behavior for the 1/11 is in contrast to that observed for the smaller species. A fragment peak corresponding to the copper cation is seen, as before, but here it is present only with very small intensity. Instead, the two peaks that dominate the fragmentation are 1/8, corresponding to loss of neutral C_3, and 0/11, corresponding to loss of the *neutral* copper atom. The loss of neutral C_3 was seen before only for the clusters with an even number of carbon atoms. Its appearance here suggests that for this cluster, breaking a carbon−carbon bond is at least comparable in energy to breaking the carbon−copper bond. Additionally, the formation of the 1/8 is the first time a fragment with an even number of carbon atoms is seen. The carbide fragments seen in Figure 3 all had an odd number of carbons. The 1/8 species formed here was not especially abundant in the mass spectrum. Apparently the tendency to lose C_3 from this cluster is strongly favored energetically and proceeds even if the mixed carbide cation formed does not contain an odd number of carbons.

The other change in fragmentation behavior for the 1/11 is the appearance of C_{11}^+ as the most intense fragment in the mass spectrum, which can only be produced by elimination of neutral copper. This is the first species for which a pure carbon cation fragment is seen. Previous mass spectrometry and dissociation experiments on pure carbon clusters have often recognized C_{11}^+ as a prominent mass peak, possibly due to its enhanced stability, a low IP, or both.[6,7] The appearance of C_{11}^+ as a charged product would usually mean that its IP is lower than that of the copper atom, which is 7.73 eV.[92] The IP of C_{11} has been measured by charge transfer bracketing (CTB) to be 7.45 eV,[70] and by vacuum ultraviolet photoionization (VUV-PI) to be 9.4 eV.[73] DFT calculations found an IP of 7.6 eV for the cyclic structure and 8.6 eV for the linear structure,[71] indicating that the discrepancy between the two experimental values was due to the measurement of the cyclic isomer in the CTB study and the linear isomer in the VUV-PI study. (The CTB study examined charge exchange processes beginning with the cation, while the VUV-PI study examined the ionization of *neutral* carbon clusters.) In the present case, the observation of C_{11}^+ and its implied low IP would suggest that it is formed as the cyclic isomer. A possible caveat to this is that dissociation could take place out of an excited state of CuC_{11}^+, and then the charged C_{11}^+ could be produced even if its IP is higher than that of Cu.

However, ion mobility experiments on pure carbon cations found only the cyclic C_{11}^+ isomer, concluding this to be the most stable structure for this ion.[82] It makes sense then that the dissociation here could produce the cyclic C_{11}^+ isomer, and that this would be the energetically favorable channel for ground electronic state dissociation of CuC_{11}^+.

The 1/12 fragmentation proceeds largely as expected when compared to the smaller even-carbon clusters. It loses C_3 and C_5 to form 1/9, and 1/7, respectively. Also, like 1/11, it produces some C_{12}^+, which indicates that the IP of this fragment is also likely lower than that of copper, or that some excited state dissociation occurs, using the arguments above. The IP of C_{12} has been measured by CTB[70] and VUV-PI[73] to be about 8.5 eV, and DFT predicts the IPs of both the linear and cyclic isomers to be in this range.[71] Thus no assignment of the structure of this fragment is possible. The 1/12 also appears to be unique in that it loses CuC to form C_{11}^+. This may be due to the fact that C_{11}^+ seems to have a special stability compared to other carbon clusters. Additionally, previous experiments have observed the loss of both C_1 and C_2 as minor (but important) fragmentation channels for C_{12}^+, possibly because of excess internal energy in some fraction of the ion distribution.[74,78b] Thus the appearance of the C_{11}^+ fragment from 1/12 is not as anomalous as it first appears.

The fragmentation for the 1/13 ion is very similar to that of 1/11. It loses C_3 to form the 1/10, or copper atom to form C_{13}^+. In this case, the results of the CTB[70] and VUV-PI,[73] when compared to the DFT calculations,[71] seem to show an IP of around 9.3 eV for the linear species and 8.09 eV for the cyclic isomer of the pure carbon cluster. Because the IP of the cyclic structure is much closer to the IP of copper atom than the linear isomer, and because in this size regime the cyclic structures of carbon clusters are strongly favored over the linear chains, it is tempting to assign a cyclic structure to our observed C_{13}^+ fragment. Again, this is consistent with ion mobility measurements which only detected the cyclic isomer for C_{13}^+.[82]

In each of these three systems, the observation of both Cu^+ and also the C_n^+ ion, which must be accompanied by the loss of neutral copper, is somewhat surprising. The Cu^+ may be coming via the sequential fragmentation of the intermediate fragments. For example, Figure 3 shows that Cu^+ does indeed come from the fragmentation of 1/8, 1/9, and 1/10, all of which are intermediates here. However, the Cu^+ could also come directly from the CuC_n^+ parent ion in a channel parallel to the most probable $C_n^+ + Cu$ route. Because the fragmentation processes here are likely multiphoton in nature, it is likely that the parent cluster ions obtain a distribution of internal energy, with some population in excited electronic states. Many of these species may fragment on the ground electronic state, likely leading to the $Cu + C_n^+$ products, while others may dissociate out of an excited state leading to $Cu^+ + C_n$.

Figure 5 shows fragmentation spectra for the 1/14, 1/15, 1/16, and 1/20 copper−carbide cations. For the most part, these cluster ions continue the patterns seen in Figure 4. They each have channels corresponding to the loss of C_3, and they also each have a channel of C_n^+ formation, corresponding to the loss of neutral Cu. The Cu^+ fragment is present as a small signal for each system, as noted above. The only other prominent fragments are C_{11}^+ from the 1/16 parent and C_{15}^+ from the 1/20 parent. As mentioned above, C_{11}^+ is known to be an abundant cluster in mass spectra of carbon, and it has indeed been seen as a sizable photofragment from C_{12}^+, C_{14}^+, and C_{16}^+,[74,78b] so its appearance as a fragment from these clusters in our experiment is not surprising. As shown in Figure 4, C_{11}^+ is a strong fragment from 1/11, which is also present in these spectra, and so it is likely that it is coming here by sequential fragmentation. Likewise, in the upper trace, C_{15}^+ is known as a fragment from C_{20}^+, and so this could also come by sequential fragmentation.

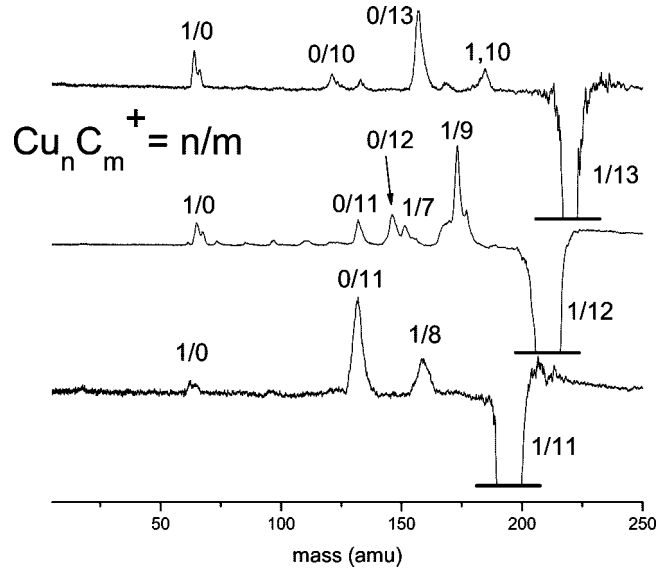

Figure 4. Photodissociation mass spectra of copper carbide clusters CuC_{11-13}^+ at 355 nm.

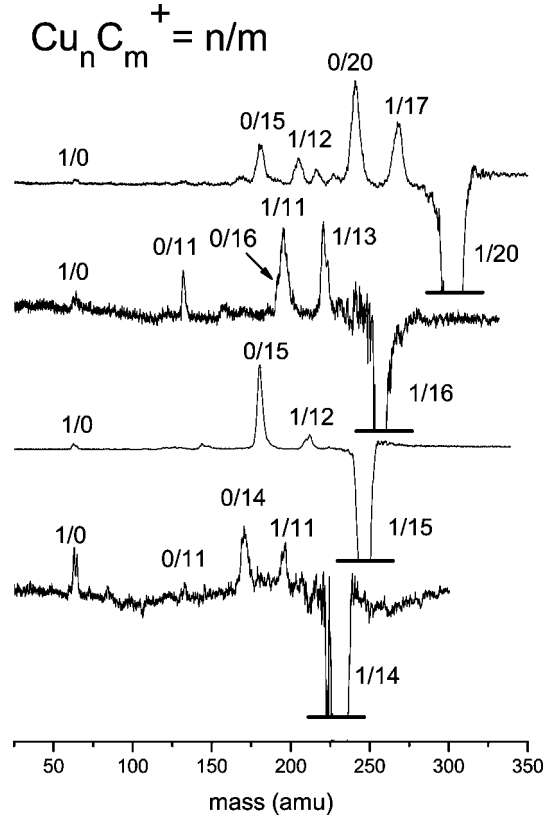

Figure 5. Photodissociation mass spectra of copper carbide clusters $CuC_{14-16,20}^+$ at 355 nm.

Transition metal carbides in this general size range have been studied previously with photodissociation and collisional dissociation.[15−18,20,21] In studies on met-cars and nanocrystals of the early transition metals,[17,18] the clusters had integrated metal−carbon frameworks with near 1:1 stoichiometries. Because of the strong metal−carbon bonding, these systems

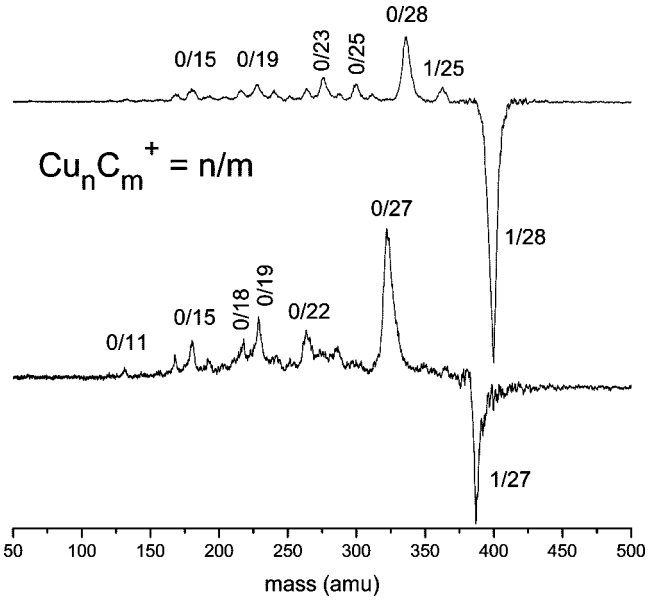

Figure 6. Photodissociation mass spectra of copper carbide clusters $CuC_{27,28}^+$ at 355 nm.

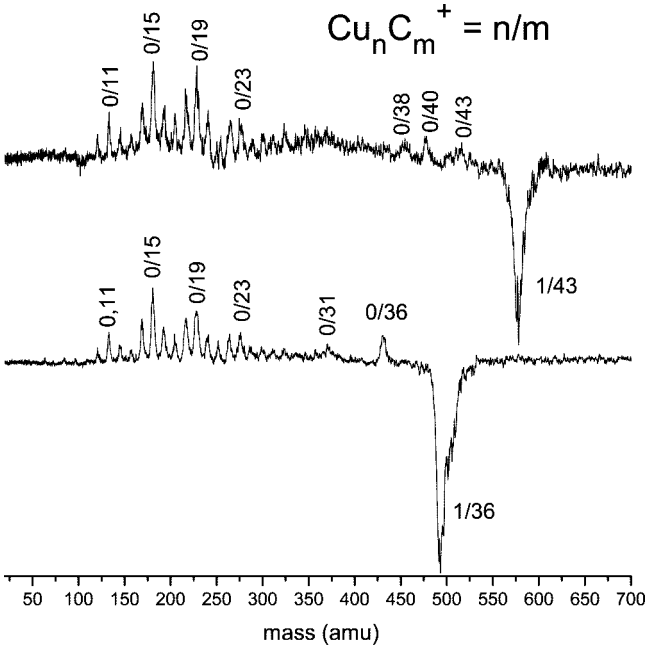

Figure 7. Photodissociation mass spectra of copper carbide clusters $CuC_{36,43}^+$ at 355 nm.

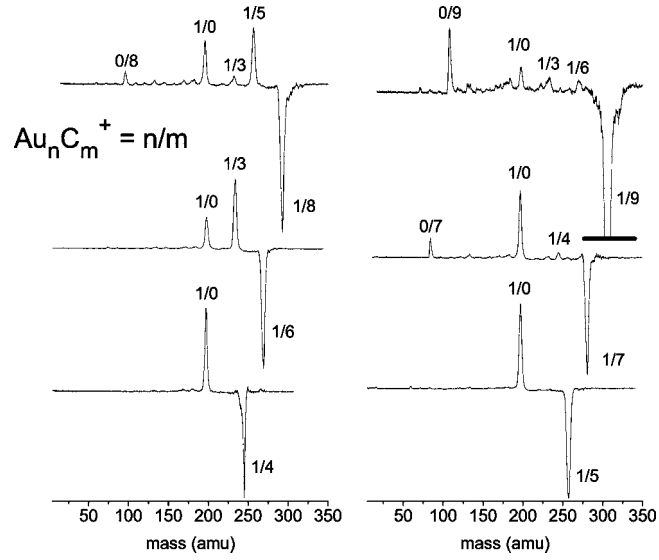

Figure 8. Photodissociation mass spectra of gold carbide clusters AuC_{4-9}^+ at 355 nm.

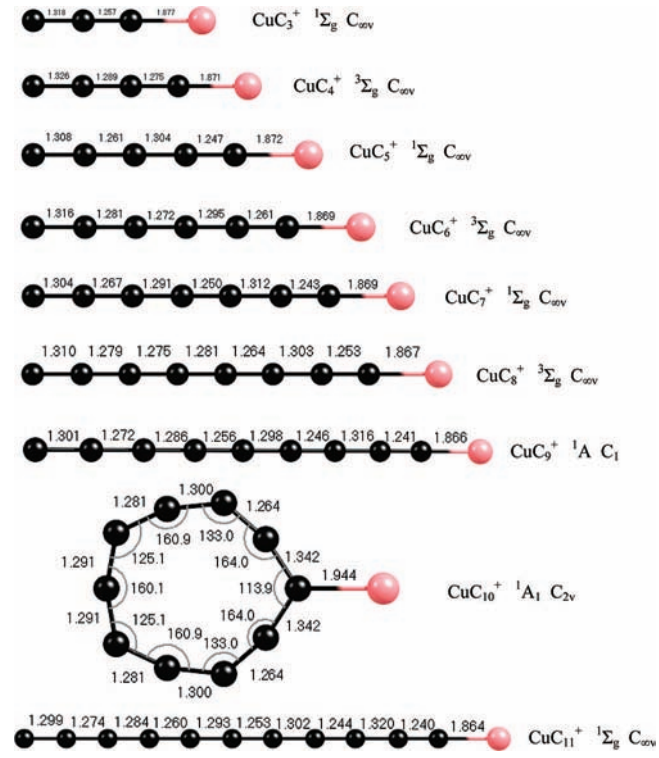

Figure 9. Calculated structures of the lowest energy isomers for copper carbide clusters CuC_{3-11}^+.

dissociated by the loss of metal or metal−carbide species; there was no loss of pure carbon molecules.[17,18] In perhaps the only other fragmentation study of small carbon-rich carbides, McElvany and Cassady investigated tantalum carbide ions with CID.[15] The dominant fragment channel for most of the $Ta_mC_n^+$ species ($m = 1-3$) smaller than $n = 9$ was the loss of neutral C_3. Additionally, some larger clusters (e.g., TaC_{10}^+) eliminated neutral C_{10}. The elimination of pure carbon species in that work was interpreted to arise because the metal−carbon bonds (estimated at 5−6 eV) were stronger than the carbon−carbon bonds.[15] As described above, the bonding between noble metals and carbon should be weaker than this, but we still observe the loss of C_3 from many cluster sizes. On the other hand, we also see the loss of the entire carbon cluster, either as a neutral or a cation, as a fragmentation channel for every species studied. However, the loss of neutral C_{10} seen by McElvany is not found in our data. Carbon forms different isomers depending on the cluster growth conditions,[6,7,82] and tantalum bonding to carbon may be quite different from that of the noble metals, so some differences between these two experiments are not surprising. The propensity for C_3 elimination in both systems, as well as in the fragmentation of pure carbon clusters, demonstrates the extremely high stability of this triatomic.

The photodissociation behavior of the metal carbides in this size regime can also be compared to the photodissociation of MSi_n^+ clusters (M = Ag, Au, and Cr).[85] In that study the most common fragmentation channel was loss of the metal atom, which would be expected for an intact silicon cluster that had metal bound to its surface. For $CrSi_{15}^+$ and $CrSi_{16}^+$, however, the major loss channel was elimination of a silicon atom. This

result suggested that the metal atom was encapsulated inside the silicon cluster, a picture that was supported by several theoretical studies. Another possibility, however, was surface-bound metal with a particularly strong metal−silicon bond. In our small metal carbide experiments, the three-dimensional structures favored by silicon are not expected. As shown below, chain and ring structures are most likely for these small carbide systems, similar to the structures found for pure carbon clusters. However, the fragmentation channels seen so far (loss of C_3, C_n, or C_n^+) could conceivably come from either linear chain or cyclic parent ions, and so these dissociation patterns alone do not provide insights into the specific structures of different sized clusters.

Figure 6 shows the photodissociation mass spectra of the 1/27 and 1/28 copper carbides. The dominant fragmentation channel for both of these species is the loss of a neutral copper atom to leave a charged carbon cluster, C_n^+. After this, lower mass carbon ions fall in decrements of C_3 and C_5 down from this, consistent with the continued fragmentation of the initially produced C_n^+ via known fragmentation routes for pure carbon cluster ions.[6,7,74,78] The C_{11}^+, C_{15}^+, C_{19}^+, and C_{23}^+ peaks tend to stand out among the other fragments, also consistent with the dissociation of pure carbon clusters of this size.[6,7,74,78] Additionally, the even−odd alternation in fragmentation behavior seen before in the smaller clusters is still somewhat noticeable. The 1/28 and 1/30 (not shown), with even numbers of carbon atoms, both show some loss of C_3 to form the mixed 1/25 or 1/27 fragment ions. The 1/27 parent, however, with an odd number of carbon atoms, produces no mixed fragments. Thus it appears that even at these larger sizes the metal−carbon binding is stronger in clusters with an even number of carbons. The fact that C_3 loss is favored in subsequent fragmentation events also suggests that these are not metal−fullerenes. C_3 is the fragment expected from linear or cyclic species, whereas fullerenes fragment by the loss of C_2.[80,82] Additionally, fullerenes are not expected to form readily at cluster sizes smaller than C_{32}, and are not the dominant isomer until $\sim C_{50}$.[68,80,82]

Figure 7 shows the photodissociation mass spectra of the 1/36 and 1/43 copper carbide clusters. Although these masses are not evident in the mass spectrum in Figure 1, they can be obtained with reasonable intensity by using the 0.5 in. diameter growth channel conditions and adjusting the spectrometer focusing for higher masses. Both of these species fragment by the loss of copper atom to give charged fragments of pure carbon. The subsequent fragmentation of the carbon clusters proceeds as expected, with losses of both C_3 and C_5. Very few fragmentation products in the size range of 30 carbons are observed, consistent with the previous observations of Smalley and co-workers from photodissociation experiments of large carbon and fullerene clusters.[68] Around C_{27}^+, peaks are observed again at essentially every carbon cluster mass, and as before the C_{11}^+, C_{15}^+, C_{19}^+, and C_{23}^+ peaks are the most prominent. Again, because we do not see any loss of C_1 or C_2 units, we conclude that the peaks here do not represent metals bound to fullerenes. Additionally it should be noted that the 1/36, which contains an even number of carbon atoms, does not show any loss of C_3 to form a mixed carbide fragment. Apparently at this large size the metal−carbon bond has become weak enough so that it always breaks, or alternatively the 1/33 species, which would be produced by loss of C_3, is not stable enough to make this fragmentation channel active.

Figure 8 shows the photodissociation spectra for the gold carbides 1/4−1/9. We were only able to obtain fragmentation spectra for the small parent ions because of the low signal levels and dissociation yields. However, these small clusters fragment in much the same way as the small copper carbides. As seen in Table 1, the 1/3, 1/4, and 1/5 for both metals apparently fragment by the loss of C_3, C_4, and C_5 neutrals, respectively, to leave only the metal cation, Au^+. The atomic metal ion is also the most prominent fragment for the 1/7 parent, and this fragment is seen with moderate intensity for each of the other parent ions studied. Additional strong fragments from each of these $1/n$ gold carbide ions include the $1/(n-3)$ species, apparently formed by the elimination of C_3. This is particularly noticeable for the 1/9 parent ion, where there seems to be a sequence of fragments corresponding to the loss of first one and then additional C_3 species. The final general kind of fragment seen for some of these gold carbides is production of the C_n^+ ion, corresponding to the loss of a neutral gold atom. This channel is seen for the 1/7 parent ion and all those with more carbon atoms than this.

The channel corresponding to the loss of neutral gold atom and the formation of the C_n^+ charged carbon cluster begins to appear at the cluster size of 1/7. Following the arguments outlined earlier, we expect that the charge in these dissociation processes will generally be on the lower IP fragment. Therefore, the IP of C_7 produced here should be less than that of the gold atom (9.225 eV).[92] High level ab initio calculations performed on C_7 predicted IPs of 9.1 eV for the cyclic isomer and 10.4 eV for the linear isomer.[73] The experimental IP values for C_7, 8.09 eV from CTB[71] and 10.1 eV from VUV-PI experiments,[73] were interpreted to come from cyclic and linear isomers, respectively. The simplest interpretation of our fragmentation, therefore, is that we are detecting the cyclic isomer of C_7^+ as the photofragment here. However, as discussed earlier, dissociation from excited electronic states of a linear species might also give this C_7^+ fragment. Ion mobility results for C_7^+ found the cyclic isomer to be more abundant than the linear one, but both structures were present.[82] The 1/8 parent ion also produces C_8^+ as a fragment, but both cyclic and chain isomers of C_8 are expected to have IP values lower than that of the gold atom.[71,73] C_9 is expected to have an IP of about 8.8 eV for the cyclic species and 9.6 eV for the linear chain, and so the C_9^+ fragment from 1/9 is therefore also most likely a cyclic species.

In much the same way seen for copper, the formation of mixed cluster fragments in the gold system is more pronounced for the clusters with an even number of carbon atoms. This is particularly true for the 1/6 and 1/8 parent ions, which have the loss of C_3 as the major channel. Compared to this, the 1/5, 1/7, and 1/9 species have only weak or nonexistent signals in the corresponding mass channels, and fragment more efficiently by the loss of metal. As noted above for copper, this implies that the metal−carbon bonds in these even-numbered systems are stronger on average. The diatomic carbide has been predicted by theory to contain one of the strongest known bonds to gold.[42,43] Although it may give rise to a dissociation energy as great as 3.5 eV,[42,43] this bonding is still expected to be weaker than that for pure carbon clusters. CID has measured the threshold dissociation energies of C_7^+ and C_8^+ to be 6.3 and 5.3 eV, respectively.[79] Nevertheless, the efficient fragmentation by the loss of C_3 to leave a mixed metal−carbon cluster does suggest that the gold has a strong effect on the bonding in these systems.

A final interesting aspect of these gold−carbide dissociation processes is in the behavior of the 1/9 species. Although the signals are weak, this cluster appears to eliminate a sequence of C_3 species, forming the 1/6, 1/3, and 1/0 fragments. Perhaps related to this, we noted above that the mass spectrum of the ions produced from the source has a noticeable discontinuity

after the 1/3, 1/6, 1/9, and 1/12 ions, as well as for the 2/3 and 2/6 ions. These combined observations raise the intriguing possibility that one isomeric form for these clusters might involve a central gold atom (or dimer) with C_3 ligands. Again, however, the mass spectra and fragmentation data alone are not enough to prove this and additional theoretical and spectroscopic work is necessary to test this fascinating suggestion.

Theoretical Results

To investigate the stability and energetics of various isomers which may be present in these experiments, we have performed DFT calculations on the cationic copper carbide clusters 1/3−1/11 and the corresponding neutral species 1/3−1/6. We have also calculated the metal−carbon binding energies for the linear cation species 1/3−1/6. The full details of these calculations are presented in the Supporting Information. We use the results of several previous computational studies on carbon-rich metal carbides to guide this study. Unfortunately, most of the previous theoretical work on the noble metal carbides has focused on diatomic and triatomic species. In studies on larger clusters, Hall and co-workers investigated palladium and platinum carbide cations with density functional theory, finding that for both metals the linear chains were the lowest energy isomer up to the size MC_9^+.[27] At larger sizes closed ring (metal bound to two atoms of a cyclic carbon cluster), open ring (metal incorporated into a carbon ring), and one-carbon ring (metal bound to one atom of a cyclic carbon cluster) structures were all found to be stable. The stability of cyclic structures for species with 10 carbon atoms is perhaps not surprising, because pure carbon clusters energetically favor rings beginning at C_{10}.[6,7] Recently Largo and co-workers also used DFT to study vanadium-doped carbon clusters, examining both linear and cyclic structures for neutral, cationic, and anionic species.[39g] They also found stable linear structures, but only for the n = 5−7 sizes was the linear isomer lowest in energy. A fan-type cyclic structure was lowest for the 1/2 and 1/4 clusters, while 1/3 and 1/8 favored the open ring structure with the vanadium incorporated into the carbon unit. A similar study of cobalt carbide cations (CoC_{1-8}^+) identified stable linear, cyclic, and fan isomers, but the linear structure was lowest in energy for all clusters other than CoC_2^+.[39j] The bonding of copper to carbon will likely be different from that of the metals studied before, but the stable geometries identified before were used to guide our search for structures in the present study.

Figure 9 shows the lowest energy structures determined here for the copper−carbon cations. The lowest energy isomer for the smaller clusters is a linear carbon chain with a copper atom attached to the end. The metal−carbon bond is the longest in these clusters, and is on the order of 1.87 Å. This is also close to the bond lengths found for metal−carbon bonds in V, Pt, and Pd carbides, all of which were 1.85−2.0 Å.[27,39] An even−odd alternation is found for both the structures and the multiplicities of these linear clusters. Most of the odd-numbered species have $^1\Sigma_g$ ground states (1/9 is ^{1}A) and exhibit acetylenic (·C≡C−C···C≡C·) bonding with alternating long and short bonds along the carbon chain. The even-numbered species, however, have $^3\Sigma_g$ ground states and cumulenic (:C=C···C=C:) bonding with a smaller alternation in bond lengths between adjacent carbons. The exceptions to the linear structure are 1/9, which is slightly bent (C_1 symmetry), and 1/10. 1/10 has a closed carbon ring structure with the copper bound to a single carbon, and this is more stable by 20.64 kcal/mol than the linear isomer. This closed ring structure has a $^1A_1$ ground state with C_{2v} symmetry. In the terminology of Hall and co-workers, which we adopt here, this is the one-carbon ring.[27] As noted above, C_{10} itself is also much more stable in a cyclic structure,[6,7,73] so the cyclic 1/10 structure is not too surprising.

Trends can also be seen in the lowest energy cyclic structures, which are found, with the exception of the 1/10 cluster, to be higher in energy than the linear isomers. The structural patterns here also exhibit an even−odd alternation. In the even clusters 1/4−1/10, the lowest energy cyclic isomer is always the one-carbon ring. The 1/4 has a $^3A_1$ ground state and 1/6 has a $^1A_1$ ground state, both with C_{2v} symmetry, 1/8 has a $^1A'$ ground state with C_s symmetry, and 1/10 has a $^1A_1$ ground state with C_{2v} symmetry. The metal−carbon bond lengths in these species are 1.91−1.93 Å. The 1/3 species is the only stable odd-numbered cyclic isomer with the one-carbon ring structure, having a $^3A'$ ground state with C_s symmetry. For the odd clusters larger than the 1/3, the lowest energy cyclic isomer is the so-called open ring, with the metal inserted into the carbon ring. The metal−carbon bonds are much longer than the carbon−carbon bonds, as expected, and range in length from 1.881 Å for 1/11 to 2.062 Å for 1/5. For the 1/5, 1/9, and 1/11 clusters, the open ring isomer has a $^1A_1$ ground state, while 1/7 has a $^1A'$ state. Even though 1/11 is more stable as a linear chain, the open ring isomer is only 8.75 kcal/mol higher in energy, by far the smallest linear−cyclic energy difference of any of these systems.

While these computations show interesting differences between the even- and odd-numbered clusters for both the linear and cyclic isomers, and the photodissociation data also show an alternation in fragment channels, the structures themselves do not necessarily reveal the source of the differences in fragmentation behavior. To gain more insight into this issue, copper−C_n dissociation energies were computed for the linear isomers for the 1/3−1/6. Surprisingly, these results also display a dramatic even−odd alternation, and do in fact help to explain the fragmentation data. The 1/3 and 1/5 were found to have copper−carbon dissociation energies of 2.35 and 2.87 eV respectively. These are well below the expected carbon−carbon bond energies, which are 5−7 eV.[76,79] Thus the fragmentation of these species by the loss of copper is understandable. For the 1/4 and 1/6 species, however, the copper−carbon dissociation energies are calculated to be much greater, at 7.00 and 7.21 eV. This is comparable to, or greater than, the expected carbon−carbon bonding. In light of these energetics, the breaking of carbon−carbon bonds and the corresponding elimination of C_3 from the small even-numbered clusters also makes sense. This, combined with the fact that C_3 loss from an even-numbered cluster leaves behind the 1/3, 1/5, 1/7, and 1/9 species, which were prominent cations in the initial mass spectrum, satisfactorily explains the even−odd alternation in fragmentation patterns observed.

The simplest picture of the copper−carbon clusters consistent with the dissociation patterns and theory, therefore, is that the smaller copper−carbon clusters have linear structures with copper on the end of the chain. The even−odd alternation in fragmentation channels comes from the alternation in electronic structure, which gives rise to stronger metal−carbon bands for the even-numbered species. The larger copper−carbon clusters also lose C_3 and the C_5 elimination channel gradually becomes more noticeable. This behavior is also found for pure carbon clusters, which have cyclic structures in the n = 10−20 size range. Additionally, the observation of C_{11}^+, C_{12}^+, and C_{13}^+ fragment ions from the respective 1/11, 1/12, and 1/13 parents suggested that these fragments were cyclic, and these could easily come from cyclic (one-carbon ring) parent ions. This fragmentation behavior and our computations also suggest that

the copper carbides in the intermediate-to-larger size range have cyclic structures. It is well-known that fullerenes fragment by the loss of C_2 units. Since we never see this channel even in our largest clusters, we conclude that the copper−carbides do not form metallofullerenes in this size range.

We have not performed any computational studies on the gold carbides, and indeed our fragmentation data on these species are also limited. However, the fragmentation patterns in the small clusters have a similar even−odd behavior to that seen for copper, and it is likely that these species also have linear structures. The additional observation in some of the gold data for multiples of C_3 as a leaving group suggests the presence of C_3 ligands bound to a gold center. More sophisticated computational work could be done to fully investigate this possibility.

Conclusions

Copper and gold carbide cluster cations produced by laser vaporization have been investigated with time-of-flight mass spectrometry, mass-selected photodissociation, and density functional theory. The mass spectra for the copper carbides are different from those seen previously for pure carbon clusters. Here an even−odd alternation in cluster intensities is seen, and species with an odd number of carbon atoms are more abundant. This is possibly due to a higher level of reactivity for the singlet ground states of the odd cluster sizes as compared to the triplet ground states in the even clusters. The mass spectrum of the gold carbides shows drops in ion intensities after clusters with 3, 6, 9, and 12 carbons.

The photodissociation data for the copper carbides also show differences between the even and odd clusters. For the small sizes, the odd-numbered species fragment by loss of the entire neutral carbon cluster, while the even-numbered ones show significant loss of C_3, leaving behind mixed metal carbide fragments. The stoichiometries of these fragments correspond to the odd-numbered clusters which were abundant in the mass spectrum. This even−odd alternation in fragmentation behavior is observed in varying degrees for clusters as large as 1/30. The gold carbide fragmentation closely follows that of the copper carbides, with even species favoring loss of C_3 to leave mixed fragments and odd ones favoring the loss of the entire intact carbon cluster. For larger clusters of both copper and gold, the IPs of some carbon cluster fragments are low enough that upon dissociation they keep the charge and a neutral metal atom is lost. The structures of some of these carbon fragments can then be identified based on comparisons to the known IPs of the linear and cyclic isomers. Loss of C_2 is never seen as a fragmentation channel for any of the clusters studied here, indicating that fullerene formation is not occurring even in the largest cluster sizes.

DFT calculations were conducted to investigate the various isomers possible for the copper carbide clusters of the size 1/3−1/11. These studies found that the ground state for all the clusters except 1/10 is a linear carbon chain with copper on the end. The computations also showed even−odd alternations in the electronic structure. The linear isomers of the even clusters are all triplets, while the odd ones are singlets. Examination of the lowest lying cyclic isomers also shows a difference between the even and odd clusters. The even ones all form a one-carbon ring in which the copper is attached to a single carbon of a closed carbon ring, and the overall ground state of the 1/10 is the one-carbon ring. The odd clusters, on the other hand, all have an open ring structure as the lowest energy cyclic isomer. Metal−carbon dissociation energies were calculated for the linear clusters 1/3−1/6, and a dramatic difference between the even and odd clusters was seen. The odd ones have metal−carbon dissociation energies less than 3 eV, while the even ones have dissociation energies near 7.00 eV. This difference in dissociation energy explains the alternation observed in the photodissociation data. For the odd clusters, breaking the metal−carbon bond is a lower energy process than breaking a carbon−carbon bond, so this fragmentation channel is favored. For the even-numbered clusters, however, the metal−carbon bonds are evidently much stronger. Breaking a carbon−carbon bond in these species is energetically competitive with or even favored over breaking the metal−carbon bond. Additionally, C_3 elimination from even clusters leaves behind odd-numbered mixed fragments, which are suggested by the mass spectral data to have higher relative stability. These two factors combined explain the differences in the observed fragmentation channels.

Although the data are not unequivocal, the simplest interpretation of the photodissociation experiments and theory would indicate that the small carbides here have linear/chain structures with the metal atom bound at the end. Beginning at a cluster size of about 10 carbon atoms, the MC_n^+ species change over to cyclic structures with the metal bound externally to a single carbon atom. These structures represent the lowest energy configurations from theory, and they are consistent with the observed fragmentation patterns. The measurement of infrared spectra for both carbon and carbide cluster cations would be very useful to confirm these structures and to provide further insight into the effects of noble metal doping on the structures of carbon clusters. Our group is pursuing these studies.

Acknowledgment. We gratefully acknowledge the Air Force Office of Scientific Research for generous support of this work (grant no. FA9550-06-1-0028).

Supporting Information Available: Full citation of Gaussian03 for ref 86, as well as frequency, intensity, and symmetry data. This material is available free of charge via the Internet at http://pubs.acs.org.

References and Notes

(1) Oyama, S. T. *Catal. Today* **1992**, *15*, 179.
(2) Oyama, S. T., Ed. *The Chemistry of Transition Metal Carbides and Nitrides*; Blackie: Glasgow, 1996.
(3) Johansson, L. I. *Surf. Sci. Rep.* **1995**, *21*, 177.
(4) Furimsky, E. *Appl. Catal. A* **2003**, *240*, 1.
(5) Cataldo, F. *Int. J. Astrobiol.* **2003**, *2*, 51.
(6) Weltner, W., Jr.; Van Zee, R. J. *Chem. Rev* **1994**, *89*, 1713.
(7) Van Orden, A.; Saykally, R. J. *Chem. Rev.* **1998**, *98*, 2313.
(8) Dresselhaus, M. S.; Dresselhaus, G.; Eklund, P. C. *Science of Fullerenes and Carbon Nanotubes*; Academic Press: San Diego, CA, 1995.
(9) Kadish, K. M.; Ruoff, R. S. *Fullerenes: Chemistry, Physics and Technology*; Wiley Interscience: New York, 2000.
(10) Chupka, W. A.; Berkowitz, J.; Giese, C. F.; Inghram, M. G. *J. Phys. Chem.* **1958**, *62*, 611.
(11) De Maria, G.; Guido, M.; Malaspina, L.; Pesce, B. *J. Chem. Phys.* **1965**, *43*, 4449.
(12) Kohl, F. J.; Stearns, C. A. *J. Phys. Chem.* **1970**, *74*, 2714.
(13) (a) Haque, R.; Gingerich, K. A. *J. Chem. Phys.* **1981**, *74*, 6407. (b) Gupta, S. K.; Nappi, B. M.; Gingerich, K. A. *J. Phys. Chem.* **1981**, *85*, 971. (c) Pelino, M.; Haque, R.; Bencivenni, L.; Gingerich, K. A. *J. Chem. Phys.* **1988**, *88*, 6534.
(14) Dietze, H. J.; Becker, S. *Int. J. Mass Spectrom. Ion Processes* **1988**, *82*, 47.
(15) (a) McElvany, S. W.; Cassady, C. J. *J. Phys. Chem.* **1990**, *94*, 2057. (b) Cassady, C. J.; McElvany, S. W. *J. Am. Chem. Soc.* **1990**, *112*, 4788.
(16) (a) Guo, B. C.; Kerns, K. P., Jr. *Science* **1992**, *255*, 1411. (b) Guo, B. C.; Wei, S.; Purnell, J.; Buzza, S., Jr. *Science* **1992**, *256*, 515. (c) Guo, B. C.; Castleman, A. W., Jr. *Advances in Metal and Semiconductor Clusters*; JAI Press: London, UK, 1994; Vol. 2.
(17) (a) Pilgrim, J. S.; Duncan, M. A. *J. Am. Chem. Soc.* **1993**, *115*, 6958. (b) Pilgrim, J. S.; Duncan, M. A. *J. Am. Chem. Soc.* **1993**, *115*, 9724. (c) Pilgrim, J. S.; Duncan, M. A. *Advances in Metal and Semiconductor*

Clusters; JAI Press: London, UK, 1995; Vol. 3. (d) Duncan, M. A. *J. Clust. Sci.* **1997**, *8*, 239.

(18) (a) Pilgrim, J. S.; Duncan, M. A. *J. Am. Chem. Soc.* **1993**, *115*, 4395. (b) Pilgrim, J. S.; Duncan, M. A. *Int. J. Mass Spectrom. Ion Processes* **1994**, *138*, 283. (c) Pilgrim, J. S.; Brock, L. R.; Duncan, M. A. *J. Phys. Chem.* **1995**, *99*, 544.

(19) (a) Yeh, C. S.; Afzaal, S.; Lee, S. A.; Byun, Y. G.; Freiser, B. S. *J. Am. Chem. Soc.* **1994**, *116*, 8806. (b) Yeh, C. S.; Byun, Y. G.; Afzaal, S.; Kan, S. Z.; Lee, S.; Freiser, B. S.; Hay, P. J. *J. Am. Chem. Soc.* **1995**, *117*, 4042. (c) Byun, Y. G.; Yeh, C. S.; Xu, Y. C.; Freiser, B. S. *J. Am. Chem. Soc.* **1995**, *117*, 8299. (d) Byun, Y. G.; Lee, S. A.; Kan, S. Z.; Freiser, B. S. *J. Phys. Chem.* **1996**, *100*, 14281.

(20) (a) Kerns, K. P.; Guo, B. C.; Deng, H. T.; Castleman, A. W., Jr. *J. Chem. Phys.* **1994**, *101*, 8529. (b) Kerns, K. P.; Guo, B. C.; Deng, H. T.; Castleman, A. W., Jr. *J. Phys. Chem.* **1996**, *100*, 16821.

(21) (a) Wei, S.; Guo, B. C.; Purnell, J.; Buzza, S. A.; Castleman, A. W., Jr. *J. Phys. Chem.* **1993**, *97*, 9559. (b) Purnell, J.; Wei, S.; Castleman, A. W., Jr. *Chem. Phys. Lett.* **1994**, *229*, 105. (c) Stairs, J. R.; Davis, K. M., Jr. *J. Chem. Phys.* **2002**, *117*, 4371.

(22) (a) Bowers, M. T. *Acc. Chem. Res.* **1994**, *27*, 324. (b) Lee, S.; Gotts, N. G.; von Helden, G.; Bowers, M. T. *Science* **1995**, *267*, 999.

(23) (a) Wang, L. S.; Li, S.; Wu, H. *J. Phys. Chem.* **1996**, *100*, 19211. (b) Li, S.; Wu, H.; Wang, L. S. *J. Am. Chem. Soc.* **1997**, *119*, 7417.

(24) (a) van Heijnsbergen, D.; von Helden, G.; Duncan, M. A.; van Roij, A. J. A.; Meijer, G. *Phys. Rev. Lett.* **1999**, *83*, 4983. (b) von Helden, G.; van Heijnsbergen, D.; Duncan, M. A.; Meijer, G. *Chem. Phys. Lett.* **2001**, *333*, 350. (c) van Heijnsbergen, D.; Duncan, M. A.; Meijer, G.; von Helden, G. *Chem. Phys. Lett.* **2001**, *349*, 220.

(25) von Helden, G.; Tielens, A. G. G. M.; van Heijnsbergen, D.; Duncan, M. A.; Hony, S.; Waters, L. B. F. M.; Meijer, G. *Science* **2000**, *288*, 313.

(26) (a) Dance, I. *J. Am. Chem. Soc.* **1993**, *115*, 11052. (b) Harris, H.; Dance, I. *J. Phys. Chem. A* **2001**, *105*, 3340. (c) Harris, H. H.; Dance, I. G. *Polyhedron* **2007**, *26*, 250.

(27) (a) Strout, D. L.; Hall, M. B. *J. Phys. Chem.* **1996**, *100*, 18007. (b) Strout, D. L.; Hall, M. B. *J. Phys. Chem. A* **1998**, *102*, 641. (c) Strout, D. L.; Miller, T. F., III; Hall, M. B. *J. Phys. Chem. A* **1998**, *102*, 6307. (d) Miller, T. F., III; Hall, M. B. *J. Am. Chem. Soc.* **1999**, *121*, 7389.

(28) Sosa, R. M.; Gardiol, P.; Beltrame, G. *Int. J. Quantum Chem.* **1997**, *65*, 919.

(29) (a) Roszak, S.; Balasubramanian, K. *J. Chem. Phys.* **1997**, *106*, 158. (b) Dai, D.; Roszak, S.; Balasubramanian, K. *J. Phys. Chem.* **2000**, *104*, 5861. (c) Dai, D.; Roszak, S.; Balasubramanian, K. *J. Phys. Chem.* **2000**, *104*, 9760. (d) Roszak, S.; Majumdar, D.; Balasubramanian, K. *J. Chem. Phys.* **2002**, *116*, 10238. (e) Majumdar, D.; Roszak, S.; Balasubramanian, K. *J. Chem. Phys.* **2003**, *118*, 130.

(30) (a) Sumathi, R.; Hendrickx, M. *J. Phys. Chem. A* **1998**, *102*, 7308. (b) Sumathi, R.; Hendrickx, M. *J. Phys. Chem. A* **1998**, *102*, 4883. (c) Arbuznikov, A. V.; Hendrickx, M. *Chem. Phys. Lett.* **2000**, *320*, 575.

(31) Rohmer, M. M.; Benard, M. *Chem. Rev.* **2000**, *100*, 495.

(32) Zhang, Q.; Lewis, S. P. *Chem. Phys. Lett.* **2003**, *372*, 836.

(33) (a) Hou, H.; Muckerman, J. T.; Liu, P.; Rodriguez, J. A. *J. Phys. Chem. A* **2003**, *107*, 9344. (b) Liu, P.; Rodriguez, J. A. *J. Chem. Phys.* **2003**, *120*, 5414. (c) Liu, P.; Rodriguez, J. A.; Muckerman, J. T. *J. Chem. Phys.* **2004**, *121*, 10321.

(34) Martinez, J. I.; Castro, A.; Rubio, A.; Poblet, J. M.; Alonso, J. A. *Chem. Phys. Lett.* **2004**, *389*, 292.

(35) (a) Varganov, S. A.; Gordon, M. S. *Chem. Phys.* **2006**, *326*, 97. (b) Varganov, S. A.; Dudley, T. J.; Gordon, M. S. *Chem. Phys. Lett.* **2006**, *429*, 49.

(36) Froudakis, G. E.; Mühlhäuser, M.; Andriotis, A. N.; Menon, M. *Phys. Rev. B* **2001**, *64*, 241401.

(37) (a) Bauschlicher, C. W., Jr. *Theor. Chem. Acc.* **2003**, *110*, 153. (b) Gutsev, G. L.; Andrews, L., Jr. *Theor. Chem. Acc.* **2003**, *109*, 298.

(38) (a) Noya, E. G.; Longo, R. C.; Gallego, L. J. *J. Chem. Phys.* **2003**, *119*, 11130. (b) Longo, R. C.; Alemany, M. M. G.; Fernández, B.; Gallego, L. J. *Phys. Rev. B* **2003**, *68*, 167401.

(39) (a) Redondo, P.; Barrientos, C.; Largo, A. *J. Phys. Chem. A* **2005**, *109*, 8594. (b) Redondo, P.; Barrientos, C.; Largo, A. *J. Phys. Chem. A* **2006**, *110*, 4057. (c) Rayón, V. M.; Redondo, P.; Barrientos, C.; Largo, A. *Chem. Phys. Lett.* **2006**, *422*, 289. (d) Largo, L.; Cimas, A.; Redondo, P.; Rayón, V. M.; Barrientos, C. *Chem. Phys.* **2006**, *330*, 431. (e) Rayón, V. M.; Redondo, P.; Barrientos, C.; Largo, A. *Chem. Eur. J.* **2006**, *12*, 6963. (f) Redondo, P.; Barrientos, C.; Largo, A. *J. Chem. Theory Comput.* **2006**, *2*, 885. (g) Redondo, P.; Barrientos, C.; Largo, A. *J. Mol. Struct. (THEOCHEM)* **2006**, *769*, 225. (h) Rayón, V. M.; Redondo, P.; Barrientos, C.; Largo, A. *J. Phys. Chem. A* **2007**, *111*, 6345. (i) Redondo, P.; Barrientos, C.; Largo, A. *Int. J. Mass Spectrom.* **2007**, *263*, 101. (j) Redondo, P.; Barrientos, C.; Largo, A. *Int. J. Mass Spectrom.* **2008**, *272*, 187.

(40) Puzzarini, C.; Peterson, K. A. *J. Chem. Phys.* **2005**, *122*, 084323.

(41) Li, S. F.; Xue, X.; Jia, Y.; Zhao, G.; Zhang, M.; Gong, X. G. *Phys. Rev. B* **2006**, *73*, 165401.

(42) (a) Barysz, M.; Pyykkö, P. *Chem. Phys. Lett.* **1998**, *285*, 398. (b) Pyykkö, P.; Patzschke, M.; Suupere, J. *Chem. Phys. Lett.* **2003**, *381*, 45. (c) Pyykkö, P. *Angew. Chem., Int. Ed.* **2004**, *43*, 4412. (d) Pyykkö, P. *Inorg. Chim. Acta* **2005**, *358*, 4113.

(43) Puzzarini, C.; Peterson, K. A. *Chem. Phys.* **2005**, *311*, 177.

(44) Naumkin, F. *Phys. Chem. Chem. Phys.* **2006**, *8*, 2539.

(45) Yamada, Y., Jr. *Chem. Phys. Lett.* **1993**, *204*, 133.

(46) Jin, C.; Haufler, R. E.; Hettich, R. L.; Barshick, C. M.; Compton, R. N.; Puretzky, A. A.; Dem'yanenko, A. V.; Tuinman, A. A. *Science* **1994**, *263*, 68.

(47) von Helden, G.; Gotts, N. G.; Maitre, P.; Bowers, M. T. *Chem. Phys. Lett.* **1994**, *227*, 601.

(48) (a) Clemmer, D. E.; Shelimov, K. B.; Jarrold, M. F. *J. Am. Chem. Soc.* **1994**, *116*, 5971. (b) Clemmer, D. E.; Jarrold, M. F. *J. Am. Chem. Soc.* **1994**, *116*, 8841. (c) Shelimov, K. B.; Clemmer, D. E.; Jarrold, M. F. *J. Phys. Chem.* **1995**, *99*, 11376. (d) Shelimov, K. B.; Jarrold, M. F. *J. Phys. Chem.* **1995**, *99*, 17677. (e) Shelimov, K. B.; Jarrold, M. F. *J. Am. Chem. Soc.* **1996**, *118*, 1139. (f) Shelimov, K. B.; Clemmer, D. E.; Jarrold, M. F. *J. Chem. Soc., Dalton Trans.* **1996**, *5*, 567.

(49) Reddic, J. E.; Duncan, M. A. *Chem. Phys. Lett.* **1997**, *264*, 157.

(50) Gibson, J. K. *J. Vac. Sci. Technol. A* **1998**, *16*, 653.

(51) (a) Bates, S. A.; Rittby, C. M. L.; Graham, W. R. M. *J. Chem. Phys.* **2006**, *125*, 074506. (b) Kinzer, R. E., Jr.; Rittby, C. M. L.; Graham, W. R. M. *J. Chem. Phys.* **2006**, *125*, 074531. (c) Bates, S. A.; Rhodes, J. A.; Rittby, C. M. L.; Graham, W. R. M. *J. Chem. Phys.* **2007**, *127*, 064506. (d) Kinzer, R. E.; Rittby, C. M. L.; Graham, W. R. M. *J. Chem. Phys.* **2008**, *128*, 064312.

(52) Szczepanski, J.; Wang, Y.; Vala, M. *J. Phys. Chem. A* **2008**,*112*, 4778.

(53) (a) Dryza, V.; Addicoat, M. A.; Gascooke, J. R.; Buntine, M. A.; Metha, G. F. *J. Phys. Chem. A* **2005**, *109*, 11180. (b) Dryza, V.; Addicoat, M. A.; Gascooke, J. R.; Buntine, M. A.; Metha, G. F. *J. Phys. Chem. A* **2008**, *112*, 5582.

(54) (a) Wang, X. B.; Ding, C. F.; Wang, L. S. *J. Phys. Chem. A* **1997**, *101*, 7699. (b) Li, X.; Wang, L. S. *J. Chem. Phys.* **1999**, *111*, 8389. (c) Wang, L. S.; Li, X. *J. Chem. Phys.* **2000**, *112*, 3602. (d) Zhai, H. J.; Wang, L. S.; Jena, P.; Gutsev, G. L.; Bauschlicher, C. W., Jr. *J. Chem. Phys.* **2004**, *120*, 8996. (e) Alexandrova, A. N.; Boldyrev, A. I.; Zhai, H. J.; Wang, L. S. *J. Phys. Chem. A* **2005**, *109*, 562.

(55) (a) Suzuki, S.; Kohno, M.; Shiromaru, H.; Achiba, Y.; Kietzmann, H.; Kessler, B.; Gantefor, G.; Eberhardt, W. *Z. Phys. D* **1997**, *40*, 407. (b) Kohno, M.; Suzuki, S.; Shiromaru, H.; Kobayashi, K.; Nagase, S.; Achiba, Y.; Kietzmann, H.; Kessler, B.; Gantefor, G.; Eberhardt, W. *J. Electron Spectrosc. Relat. Phenom.* **2000**, *112*, 163.

(56) Tono, K.; Terasaki, A.; Ohta, T.; Kondow, T. *J. Chem. Phys.* **2002**, *117*, 7010.

(57) Knappenberger, K. L., Jr.; Jones, C. E., Jr.; Sobhy, M. A.; Iordanov, I.; Sofo, J.; Castleman, A. W., Jr. *J. Phys. Chem. A* **2006**, *110*, 12814.

(58) (a) Weiss, F. D.; Elkind, J. L.; O'Brien, S. C.; Curl, R. F.; Smalley, R. E. *J. Am. Chem. Soc.* **1988**, *110*, 4464. (b) Chai, Y.; Guo, T.; Jin, C.; Haufler, R. E.; Chibante, L. P. F.; Fure, J.; Wang, L.; Alford, J. M.; Smalley, R. E. *J. Phys. Chem.* **1991**, *95*, 7564.

(59) McElvany, S. W. *J. Phys. Chem.* **1992**, *96*, 4935.

(60) Roth, L. M.; Huang, Y.; Schwedler, J. T.; Cassady, C. J.; Ben-Amotz, D.; Kahr, B.; Freiser, B. S. *J. Am. Chem. Soc.* **1991**, *113*, 6298.

(61) Clemmer, D. E.; Hunter, J. M.; Shelimov, K. B.; Jarrold, M. F. *Nature* **1994**, *372*, 248.

(62) (a) Tast, F.; Malinowski, N.; Frank, S.; Heinebrodt, M.; Billas, I. M. L.; Martin, T. P. *Phys. Rev. Lett.* **1996**, *77*, 3529. (b) Tast, F.; Malinowski, N.; Frank, S.; Heinebrodt, M.; Billas, I. M. L.; Martin, T. P. *Z. Phys. D: At. Mol. Clusters* **1997**, *40*, 351. (c) Branz, W.; Billas, I. M. L.; Malinowski, N.; Tast, F.; Heinebrodt, M.; Martin, T. P. *J. Chem. Phys.* **1998**, *109*, 3425. (d) Malinowski, N.; Branz, W.; Billas, I. M. L.; Heinebrodt, M.; Tast, F.; Martin, T. P. *Eur. Phys. J. D* **1999**, *9*, 41. (e) Branz, W.; Malinowski, N.; Martin, T. P. *J. Chem. Phys.* **2001**, *114*, 2963.

(63) (a) Reddic, J. E.; Robinson, J. C.; Duncan, M. A. *Chem. Phys. Lett.* **1997**, *279*, 203. (b) Grieves, G. A.; Buchanan, J. W.; Reddic, J. E.; Duncan, M. A. *Int. J. Mass Spectrom.* **2001**, *204*, 223.

(64) (a) Nakajima, A.; Nagao, S.; Takeda, H.; Kurikawa, T.; Kaya, K. *J. Chem. Phys.* **1997**, *107*, 6491. (b) Kurikawa, T.; Nagao, S.; Miyajima, K.; Nakajima, A.; Kaya, K. *J. Phys. Chem. A* **1998**, *102*, 1743. (c) Nagao, S.; Kurikawa, T.; Miyajima, K.; Nakajima, A.; Kaya, K. *J. Phys. Chem. A* **1998**, *102*, 4495. (d) Nagao, S.; Negishi, Y.; Kato, A.; Nakamura, Y.; Nakajima, A.; Kaya, K. *J. Phys. Chem. A* **1999**, *103*, 8909. (e) Palpant, B.; Negishi, Y.; Sanekata, M.; Miyajima, K.; Nagao, S.; Judai, K.; Rayner, D. M.; Simard, B.; Hackett, P. A.; Nakajima, A.; Kaya, K. *J. Chem. Phys.* **2001**, *114*, 8469.

(65) Balch, A. L.; Olmstead, M. M. *Chem. Rev.* **1998**, *98*, 2123.

(66) Caraiman, D.; Koyanagi, G. K.; Scott, L. T.; Preda, D. V.; Bohme, D. K. *J. Am. Chem. Soc.* **2001**, *123*, 8573.

(67) (a) Rohlfing, E. A.; Cox, D. M.; Kaldor, A. *J. Chem. Phys.* **1984**, *81*, 3322. (b) Rohlfing, E. A. *J. Chem. Phys.* **1990**, *93*, 7851.

(68) (a) Kroto, H. W.; Heath, J. R.; O'Brien, S. C.; Curl, R. F.; Smalley, R. E. *Nature* **1985**, *318*, 162. (b) Curl, R. F.; Smalley, R. E. *Science* **1988**, *242*, 1017.

(69) Hahn, M. Y.; Honea, E. C.; Paguia, A. J.; Schriver, K. E.; Camarena, A. M.; Whetten, R. L. *Chem. Phys. Lett.* **1986**, *130*, 12.

(70) (a) Bach, S. B. H.; Eyler, J. R. *J. Chem. Phys.* **1990**, *92*, 358. (b) Ramanathan, R.; Zimmerman, J. A.; Eyler, J. R. *J. Chem. Phys.* **1993**, *98*, 7838.

(71) Giuffreda, M. G.; Deleuze, M. S.; Francois, J. P. *J. Phys. Chem. A* **1999**, *103*, 5137.

(72) (a) Wakabayashi, T.; Momose, T.; Shida, T. *J. Chem. Phys.* **1999**, *111*, 6260. (b) Kato, Y.; Wakabayashi, T.; Momose, T. *J. Chem. Phys.* **2003**, *118*, 5390.

(73) Belau, L.; Wheeler, S. E.; Ticknor, B. W.; Ahmed, M.; Leone, S. R.; Allen, W. D.; Schaefer, H. F., III; Duncan, M. A. *J. Am. Chem. Soc.* **2007**, *129*, 10229.

(74) (a) Geusic, M. E.; Jarrold, M. F.; McIlrath, T. J.; Bloomfield, L. A.; Freeman, R. R.; Brown, W. L. *Z. Phys. D: At., Mol. Clusters* **1986**, *3*, 309. (b) Geusic, M. E.; McIlrath, T. J.; Jarrold, M. F.; Bloomfield, L. A.; Freeman, R. R.; Brown, W. L. *J. Chem. Phys.* **1986**, *84*, 2421. (c) Geusic, M. E.; Jarrold, M. F.; McIlrath, T. J.; Freeman, R. R.; Brown, W. L. *J. Chem. Phys.* **1987**, *86*, 3862.

(75) O'Brien, S. C.; Heath, J. R.; Curl, R. F.; Smalley, R. E. *J. Chem. Phys.* **1988**, *88*, 220.

(76) Sowa, M. B.; Hintz, P. A.; Anderson, S. L. *J. Chem. Phys.* **1991**, *95*, 4719.

(77) Bouyer, R.; Roussel, F.; Monchicourt, P.; Perdix, M.; Pradel, P. *J. Chem. Phys.* **1994**, *100*, 8912.

(78) (a) Pozniak, B.; Dunbar, R. C. *Int. J. Mass Spectrom. Ion Processes* **1994**, *133*, 97. (b) Pozniak, B. P.; Dunbar, R. C. *Int. J. Mass Spectrom. Ion Processes* **1997**, *165/166*, 29.

(79) Sowa-Resat, M. B.; Hintz, P. A.; Anderson, S. L. *J. Phys. Chem.* **1995**, *99*, 10736.

(80) (a) Radi, P. P.; Bunn, T. L.; Kemper, P. R.; Molchan, M. E.; Bowers, M. T. *J. Chem. Phys.* **1988**, *88*, 2809. (b) Radi, P. P.; Hsu, M. T.; Brodbelt-Lustig, J.; Ricon, M.; Bowers, M. T. *J. Chem. Phys* **1990**, *92*, 4817.

(81) (a) Gluch, K.; Matt-Leubner, S.; Echt, O.; Concina, B.; Scheier, P.; Mark, T. D. *J. Chem. Phys.* **2004**, *121*, 2137. (b) Concina, B.; Gluch, K.; Matt-Leubner, S.; Echt, O.; Scheier, P.; Mark, T. D. *Chem. Phys. Lett.* **2005**, *407*, 464.

(82) (a) von Helden, G.; Hsu, M. T.; Kemper, P. R.; Bowers, M. T. *J. Chem. Phys.* **1991**, *95*, 3835. (b) von Helden, G.; Hsu, M. T.; Gotts, N.; Bowers, M. T. *J. Phys. Chem.* **1993**, *97*, 8182. (c) von Helden, G.; Gotts, N. G.; Bowers, M. T. *J. Am. Chem. Soc.* **1993**, *115*, 4363.

(83) (a) France, M. R.; Buchanan, J. W.; Robinson, J. C.; Pullins, S. H.; Tucker, J. L.; King, R. B.; Duncan, M. A. *J. Phys. Chem. A* **1997**, *101*, 6214. (b) Molek, K. S.; Jaeger, T. D.; Duncan, M. A. *J. Chem. Phys.* **2005**, *123*, 144313. (c) Molek, K. S.; Reed, Z. M.; Ricks, A. M.; Duncan, M. A. *J. Phys. Chem. A* **2007**, *111*, 8080. (d) Reed, Z. A.; Duncan, M. A. *J. Phys. Chem. A* **2008**, *112*, 5354. (e) Molek, K. S.; Anfuso-Cleary, C.; Duncan, M. A. *J. Phys. Chem. A* **2008**, *112*, 9238.

(84) Ticknor, B. W.; Duncan, M. A. *Chem. Phys. Lett.* **2005**, *405*, 214.

(85) Jaeger, J. B.; Jaeger, T. D.; Duncan, M. A. *J. Phys. Chem. A* **2006**, *110*, 9310.

(86) Frisch, M. J.; et al. *Gaussian 03*, Revision B.02; Gaussian, Inc.: Pittsburgh, PA, 2003 (see the Supporting Inforamtion for the full citation).

(87) Becke, A. D. *J. Chem. Phys.* **1993**, *98*, 5648.

(88) Lee, C.; Yang, W.; Parr, R. G. *Phys. Rev. B* **1988**, *37*, 785.

(89) Krishnan, R.; Binkley, J. S.; Seeger, R.; Pople, J. A. *J. Chem. Phys.* **1980**, *72*, 650.

(90) Dunning, T. H.; Hay, P. J. *Methods of Electronic Structure Theory*; Schaefer, H. F., ed.; Plenum Press: New York, 1977; Vol. 2.

(91) (a) Hay, P. J.; Wadt, W. R. *J. Chem. Phys.* **1985**, *82*, 270. (b) Hay, P. J.; Wadt, W. R. *J. Chem. Phys.* **1985**, *82*, 284. (c) Hay, P. J.; Wadt, W. R. *J. Chem. Phys.* **1985**, *82*, 299.

(92) Lias, S. G. "Ionization Energy Evaluation" in NIST Chemistry WebBook, NIST Standard Reference Database No. 69; P.J. Linstrom, Mallard, W.G., Eds.; June 2005, National Institute of Standards and Technology, Gaithersburg MD (http://webbook.nist.gov).

(93) Harrison, J. F. *Chem. Rev.* **2000**, *100*, 679.

(94) Raghavachari, K.; Binkley, J. S. *J. Chem. Phys.* **1987**, *87*, 2191.

JP807867R